Correlation energy and spin susceptibility of a two-valley two-dimensional electron gas

M. Marchi,[1,2] S. De Palo,[1,3] S. Moroni,[1,2] and Gaetano Senatore[1,3]
[1]*INFM–CNR DEMOCRITOS National Simulation Center, via Beirut 2-4, 34014 Trieste, Italy*
[2]*International School for Advanced Studies (SISSA), via Beirut 2-4, 34014 Trieste, Italy*
[3]*Dipartimento di Fisica Teorica, Università di Trieste, Strada Costiera 11, 34014 Trieste, Italy*
(Received 28 May 2009; published 1 July 2009)

We find that the spin susceptibility of a two-dimensional electron system with valley degeneracy does not grow critically at low densities, at variance with experimental results [A. Shashkin *et al.*, Phys. Rev. Lett. **96**, 036403 (2006)]. We ascribe this apparent discrepancy to the weak disorder present in experimental samples. Our prediction is obtained from accurate correlation energies computed with state-of-the-art diffusion Monte Carlo simulations and fitted with an analytical expression which also provides a local spin density functional for the system under investigation.

DOI: 10.1103/PhysRevB.80.035103 PACS number(s): 71.10.−w, 71.15.Mb, 71.45.Gm, 02.70.Ss

I. INTRODUCTION

The spin properties of low-dimensional electron systems in solid-state devices are of great interest in relation to spintronics and quantum computing,[1] both at the fundamental level and for technological applications, with the long-wavelength spin susceptibility of the two-dimensional electron gas (2DEG) playing an important role in the control of nuclear spins.[2] They are also believed to be intimately related to the apparent metal-insulator transition (MIT) observed in two dimensions.[3–7] Indeed the spin susceptibility χ_s of the 2DEG, measured with various techniques,[6] is consistently found to grow with respect to its noninteracting Pauli value χ_0 as the density is lowered and the MIT is approached.[3–5] Recently, experimental evidence has been given for a critical growth of χ_s in Si metal-oxide-semiconductor field-effect transistors (MOSFETs) at a finite density[3] coincident, within experimental uncertainties, with the critical density for the MIT.[6,7] The qualitative question which we answer in this paper is whether such a *divergence* is a property of the ideally clean two-valley (2V) 2DEG, the simplest model of electrons confined in a Si MOSFET,[8] or is due to some other factor. It should be stressed from the outset that the valley degree of freedom has qualitative effects on the 2DEG properties, making the fully spin-polarized fluid never stable,[9] at variance with the one-valley (1V) 2DEG, and importantly affects the MIT.[10,11]

Correlation plays a crucial role in the so-called EG, i.e., electrons with a $1/r$ pair potential, moving in a neutralizing charge background.[12] Its importance grows both with lowering the density and the space dimensionality, and tends to quantitatively and often even qualitatively change the predictions of simple schemes, such as the Hartree-Fock (HF) or the random-phase approximation (RPA).[12] In the low-density strongly correlated EG, which would be more properly called an electron liquid, the energy balance determining the system properties is played on a very minute scale and, to get meaningful predictions, a great accuracy such as the one afforded by quantum Monte Carlo (QMC) methods is necessary.[12]

QMC simulations have provided over the years the method of choice for microscopic studies of the 2DEG,[9,13–17] which has recently shown providing a rather accurate model for electrons confined in solid-state devices.[18] However, no QMC prediction is available for χ_s in the 2V2DEG, and other theoretical estimates, obtained either in RPA (Refs. 19 and 20) or with a classical mapping,[21] do not appear reliable.[22] Here, to calculate χ_s we resort to extensive state-of-the-art simulations of the 2V2DEG, using the diffusion Monte Carlo (DMC) technique.[23] We thus obtain the dependence of the ground-state energy on both the density and the spin polarization, also improving on Ref. 9, with the use of twist-averaged boundary conditions (TABCs) (Ref. 24) and trial wave functions including backflow (BF).[14]

II. CORRELATION ENERGY OF THE 2V2DEG

In the 2V2DEG, electrons possess an additional discrete degree of freedom, i.e., the valley flavor or index, which can be conveniently described with a pseudospin. One may identify electrons with given spin and pseudospin indexes as belonging to a species or *component*. Accordingly, the paramagnetic 2V2DEG is a four-component system while both the fully spin-polarized 2V2DEG and the paramagnetic 1V2DEG have two components. For the sake of simplicity, we restrict here to the symmetric case where the number of electrons and the spin polarization are the same for both valleys.[25] Thus, at zero temperature, the state of the system is fully specified by the coupling parameter $r_s=1/\sqrt{\pi n a_B}$ and the spin polarization $\zeta=(n_\uparrow-n_\downarrow)/n$, with n as the total electron density, a_B as the Bohr radius, and $n_{\uparrow(\downarrow)}$ as the density of up-spin (down-spin) electrons. Below, Rydberg units are used throughout.

A. Simulation details

We have performed simulations with the fixed-phase (FP) (Ref. 26) DMC method, which gives the lowest upper bound to the ground-state energy consistent with the many-body phase of a suitably chosen complex-valued trial function. For real trial functions, FP DMC reduces to the standard fixed-node (FN) approximation.[23] A complex trial function allows using TABCs,[24] which reduce the size dependence of the kinetic energy by one order of magnitude with respect to periodic boundary conditions (PBC). Furthermore, since

TABCs do not require closed shells in k space, there are no restrictions on the number of electrons per component so that the polarization can be changed by flipping any number of spins, with fixed total number of electrons.[27] Our trial function is the product of Slater plane-wave (PW) determinants (one per component) and a Jastrow factor.[15] BF correlations[14] are included only for $\zeta=0$ and $\zeta=1$ but with FN DMC and in PBC. Their contribution to the ground-state energy is then added to the PW energies assuming a quadratic dependence on polarization as in Refs. 16 and 17. The ground-state energy per particle $E_N(r_s,\zeta)$, calculated for several values of r_s, ζ, and the electron number N, is recorded in Table III of Appendix A.

B. Analytic representation

Following Ref. 17, we determine the energy per particle $E(r_s,\zeta)$ in the thermodynamic limit by fitting to the data listed in Table III an analytic expression which embodies the r_s and ζ dependence as well as a Fermi-liquid-type size correction

$$E_N(r_s,\zeta)=E(r_s,\zeta)+\Delta T_N(r_s,\zeta)+(\eta+\eta_z\zeta^2)\frac{1}{r_sN}+(\gamma+\gamma_z\zeta^2)\frac{1}{(r_sN)^{3/2}}. \quad (1)$$

The fitting parameters η, η_z, γ, and γ_z take into account potential-energy finite-size effects, while $\Delta T_N(r_s,\zeta)$ is the difference of the noninteracting kinetic energy evaluated at finite N with TABCs and in the thermodynamic limit. $E(r_s,\zeta)$ is customarily decomposed as sum of the noninteracting kinetic energy, $\epsilon_0(r_s,\zeta)=(1+\zeta^2)/(2r_s^2)$, the exchange energy, $e_x(r_s,\zeta)=-\frac{4}{3\pi}\frac{1}{r_s}[(1+\zeta)^{3/2}+(1-\zeta)^{3/2}]$, and the unknown correlation energy $e_c(r_s,\zeta)$, for which we adopt the same analytical representation of Ref. 17,

$$e_c(r_s,\zeta)=(e^{-\beta r_s}-1)e_x^{(6)}(r_s,\zeta)+\sum_{i=0,2}\zeta^{2i}\alpha_i(r_s), \quad (2)$$

where $e_x^{(6)}(r_s,\zeta)=e_x(r_s,\zeta)-(1+\frac{3}{8}\zeta^2+\frac{3}{128}\zeta^4)e_x(r_s,0)$ and the functions $\alpha_i(r_s)$ are defined by

$$\alpha_i(r_s)=A_i+(B_ir_s+C_ir_s^2+D_ir_s^3)\times\ln\left(1+\frac{1}{E_ir_s+F_ir_s^{3/2}+G_ir_s^2+H_ir_s^3}\right). \quad (3)$$

We constrain the correlation energy [Eq. (2)] to satisfy known high- and low-density limits (Appendix B), reducing in this way the number of free fitting parameters from 29 to 18. The correlation energy of the 2V2DEG, as given by Eqs. (2) and (3) with the parameters listed in Table I, represents a central result of this work.

C. Phase diagram

In Fig. 1 we plot the energies of the paramagnetic and the fully spin-polarized 2V2DEG. They are shown by solid lines labeled with the number of components $N_c=4$ and $N_c=2$, respectively. For comparison, we also plot QMC results for other phases of the 2DEG; $N_c=1$ labels the fully polarized one-valley 2DEG,[17] whereas the 2D charged-boson fluid[28] corresponds to the limit of an infinite-component 2DEG. The energy of the Wigner crystal is known to be almost independent of the number of components;[13,15] we report here the result of Ref. 15. We note that at large r_s as the number of components increases the ground-state energy appears to quickly approach the infinite-component limit.

TABLE I. Parameters of the analytic representation [Eqs. (2) and (3)] of the correlation energy of the 2V2DEG, determined from Eq. (1) by a least-squares fit to the data listed in Table III. The reduced chi square is $\tilde{\chi}^2=4.82$. The table footnote marks constrained parameters, whereas C_2 is fixed to zero since it turned out to be irrelevant in the fitting procedure. The parameters η, η_z, γ, and γ_z in Eq. (1) only concern the size extrapolation; their optimal values are 0.056, 0.17, 2.03, and 0.45, respectively.

	$i=0$	$i=1$	$i=2$
A_i	−0.99870[a]	0.44570[a]	0.0082290
B_i	$\frac{16}{3\pi}(10-3\pi)$[a]	−0.85288[a]	0.048979
C_i	0.62208	−7.6202	0
D_i	0.029726	−1.6194	−0.051302
E_i	1.6208	12.714	25.911
F_i	−0.012856	0[a]	0[a]
G_i	0.66150	19.692[a]	15.072[a]
H_i	0.029765[a]	3.6334[a]	6.2343[a]
β		11.879	

[a]Constrained parameters.

The dashed line for $N_c=2$ in Fig. 1 is the result of Ref. 17 for the paramagnetic 2DEG. Its agreement with our curve for

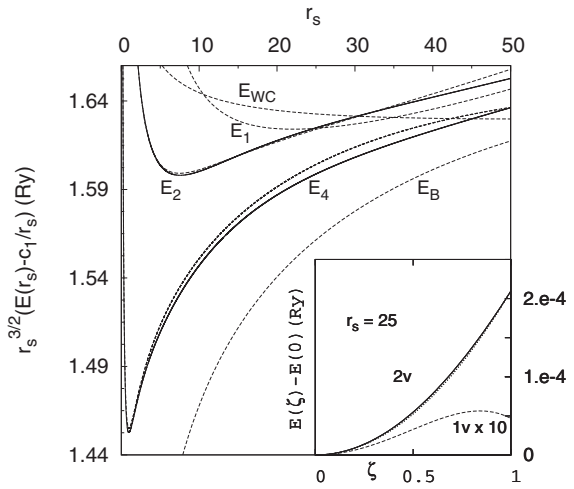

FIG. 1. Energy per particle of various phases of the 2DEG at $T=0$. The energy label indicates the number N_c of equivalent components in the homogeneous fluid, the bosonic fluid (B), or the triangular Wigner crystal (WC), as applicable. Results of the present study are given by solid lines. The dashed lines are from Ref. 17 (E_1,E_2), Ref. 9 (E_4), Ref. 15 ($E_{\rm WC}$), and Ref. 28 ($E_{\rm B}$). The inset shows $E(r_s,\zeta)-E(r_s,0)$ from Eq. (2) (solid line) together with the simple quadratic dependence $[E(r_s,1)-E(r_s,0)]\zeta^2$ (dotted) for the 2V2DEG and the result for the 1V2DEG (Ref. 17) (dashed) magnified by a factor of 10 at $r_s=25$.

TABLE II. Difference $\Delta = E_N^{BF}(r_s,\zeta) - E_N^{PW}(r_s,\zeta)$ between the BF and the PW energies (in Rydberg per particle) at selected values of r_s, ζ, N. In parentheses are the statistical error on the last digit.

	$\zeta=0$		$\zeta=1$	
r_s	N	Δ	N	Δ
1	52	−0.0028(1)	50	−0.0034(1)
			58	−0.0035(2)
			90	−0.0032(1)
2	52	−0.00166(5)	42	−0.00175(9)
			50	−0.00192(9)
			58	−0.00217(9)
5	52	−0.00057(2)	50	−0.00077(3)
			58	−0.00088(3)
10	52	−0.00021(1)	42	−0.00025(1)
	84	−0.00022(1)	50	−0.00030(2)
			58	−0.00032(2)
20	52	−0.000043(6)	42	−0.000081(7)
			50	−0.000085(7)
			58	−0.000116(6)
			90	−0.000116(6)
40	52	−0.000020(1)	50	−0.000020(1)
			90	−0.000031(1)

the polarized 2V2DEG is expected but still gratifying: the two calculations differ by details in the extrapolation to the thermodynamic limit and the closeness of their results supports a good control of the finite-size bias. The dashed line for $N_c=4$ is instead the result of Ref. 9 for the paramagnetic 2V2DEG. Its difference with the present results conveys a physical information, namely, the quantitative effect of BF correlations which were not included in the previous simulations.[9] Backflow improves the nodal structure of the PW wave function, yielding in the FN approximation a tighter upper bound to the exact ground-state energy.[14] It is known[17] that BF correlations lower the FN energy more for $N_c=2$ than for $N_c=1$. Here we find that the BF energy gain for $N_c=4$ (Ref. 29) is *smaller* than that for $N_c=2$ (see Table II of Appendix A), albeit larger than that for $N_c=1$. The modest effect of BF correlations for $N_c=4$ entails only marginal quantitative changes to the phase diagram of the 2V2DEG predicted in Ref. 9. The density of Wigner crystallization shifts to a slightly lower value, $r_s \simeq 45$.

Before discussing the spin-polarization dependence of the energy and our prediction for the spin susceptibility, we should stress that our results provide the most accurate available estimate for the correlation energy e_c of the 2V2DEG, which in turn is the key ingredient for density-functional-theory (DFT) studies of inhomogeneous two-valley systems in 2D within the local spin-density approximation.[30] The knowledge of e_c also allows one to check the accuracy of the ansatz made in Ref. 31 to construct the correlation energy of a system with an arbitrary number of components, $\epsilon_c(N_c)$, in terms of that of the one-valley system.[17] A comparison between $\tilde{\epsilon}_c(N_c)$ from Ref. 31, the present e_c, and the nominally exact QMC results for charged bosons[28] (Appendix C) exposes the limited accuracy of $\tilde{\epsilon}_c(N_c)$ especially at large r_s, including its prediction[31] of an unphysical transition between the nodeless ground state of the infinite-component system and the antisymmetric ground state of the one-component 2DEG. Yet, the comparison between DFT calculations of two-valley symmetric systems using either $\tilde{\epsilon}_c(N_c)$ or the present e_c would provide a valuable test of the adequacy of $\tilde{\epsilon}_c(N_c)$ for DFT applications.

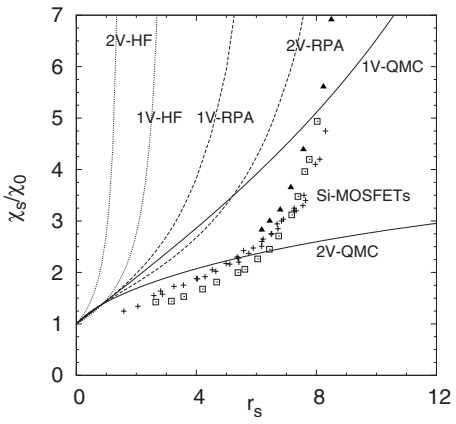

FIG. 2. Spin-susceptibility enhancement of the 1V2DEG and the 2V2DEG. The results of the present work are compared with HF and RPA (Refs. 19 and 20) predictions as well as QMC results for the one-valley case (Ref. 17). Experimental results for Si MOSFETs are also shown (Refs. 3 and 5).

Our calculations confirm the absence of a transition from the paramagnetic to the fully spin-polarized fluid in the two-valley symmetric system.[9] Moreover, in the whole density range, where the fluid is stable, we find no evidence for the stability of a state with partial spin polarization. As illustrated in Fig. 1 for $r_s=25$, $E(r_s,\zeta)$ displays its minimum at $\zeta=0$ and, for all practical purposes, can be considered a convex function of ζ.[32] Convexity ensures that, by turning on an in-plane magnetic field B, the absolute minimum displayed by the energy goes continuously from $\zeta=0$ to $\zeta=1$. If the energy exhibits a local maximum or even an inflection point for $\zeta<1$, instead, the B-driven transition to the full spin polarization becomes a first-order transition and is accompanied by a jump in the polarization.[33] This is clearly the case for the 1V2DEG at $r_s=25$ also shown in Fig. 1.

III. SPIN SUSCEPTIBILITY

The spin susceptibility enhancement[12] of the 2V2DEG is readily calculated using Eq. (2) as

$$\chi_s/\chi_0 = \left[1 - \frac{2r_s}{\pi} + 2r_s^2\alpha_1(r_s)\right]^{-1}. \tag{4}$$

In Fig. 2 we compare our QMC prediction with the available experimental results for electrons confined in Si MOSFETs. It is evident that the 2V2DEG spin susceptibility moderately overestimates experiments at high density but largely underestimates them at low density, where it does not display any critical growth. In fact χ_s is a concave function of r_s at all

densities where the fluid phase is stable. Indeed, a realistic description of a 2DEG in a solid-state device requires consideration of additional elements such as transverse thickness[18,19] and disorder scattering.[18] As the thickness is known to suppress the spin susceptibility and a weak disorder to enhance it, at present the only likely candidate to explain the experimentally observed critical behavior of χ_s (Ref. 3) appears to be a weak disorder. In Fig. 2 we also report the QMC results of a 1V2DEG.[17] It is clear that the valley degeneracy causes a substantial suppression of the spin susceptibility, in qualitative agreement with the effect found in experiments on AlAs based quantum wells[4] although for an in-plane anisotropic mass. Moreover, $\chi_s(r_s)$ changes from a convex to a concave function in going from the 1V to the 2V2DEG. We also show in Fig. 2 the predictions of HF and RPA. The general trend is that, while RPA performs somewhat better than HF, both largely overestimate the QMC predictions and yield divergences which either have no counterpart in QMC, for the 2V2DEG, or in the best case take place at a density about 13 times larger than that in QMC, for the 1V2DEG. At least RPA reverts the qualitatively wrong prediction of HF, which yields an enhancement of the spin susceptibility in going from the one- to the two-valley system.

IV. DISCUSSION AND CONCLUSIONS

We have reliably estimated the spin susceptibility of the 2V2DEG, which provides the simplest model for electrons confined in Si MOSFETs. Our results clearly point to the crucial qualitative role of weak disorder scattering in determining the critical growth found in the measured susceptibility at low density[3] and to a likely minor quantitative role of transverse thickness in suppressing the susceptibility at high density. 2D electron systems in high mobility Si MOSFETs at times have been termed *clean*, meaning in fact *without admixture of local moments*,[3] but also implicitly implying that observed properties would be disorder independent and would correspond to those of an ideally clean electron gas. This latter viewpoint, fostered by the recent experimental observation that the effective-mass enhancements of samples[34,35] with peak mobilities differing by about one order of magnitude appear to be the same within error bars (of about 10%), is contradicted by our findings. We should stress indeed that the samples of Refs. 34 and 35 are different on a number of counts and not only for the amount of disorder. Electrons in (111) Si MOSFETs (Ref. 34) have (i) a sizeable band mass anisotropy $m_x/m_y=0.28$, i.e., comparable with the one in AlAs quantum wells[36] and (ii) a transverse thickness parameter $\sqrt{(3)}b/(r_s a_B)$ (see, e.g., Ref. 18 for the definition) which is more than twice the one in (100) Si MOSFETs.[35] Both effects (mass anisotropy and thickness) are known to suppress spin susceptibility in an appreciable manner.[18,36] Moreover, comparing the absolute peak mobilities of Ref. 34 on the one hand and of Ref. 35 on the other, i.e., of systems with quantitatively different length and energy scales (due to different band masses), is not appropriate. If l and a_B are, respectively, the mean-free path and the effective Bohr radius in a given system, we find that the peak of $l/(r_s a_B)$ for the EG of Ref. 34 is only three times smaller than that of the EG of Ref. 35. Hence the experiment in Ref. 34 in our opinion is not at all conclusive in ruling out an effect of disorder on the effective mass, let alone on the spin susceptibility of these systems.

We have also obtained: an assessment of the backflow effects on the energy of the two-valley paramagnetic phase, which remains stable with respect to any partially or fully polarized phase, up to the Wigner crystallization; an analytical fit of the QMC correlation energy, which also interpolates between exact high- and low-density limits and provides a local spin density functional for DFT studies of two-valley systems; the clear indication that an accurate account of correlation beyond RPA is crucial when considering the properties of both 1V2DEG and 2V2DEG.

APPENDIX A: DETAILS OF THE DMC SIMULATIONS

The trial function was chosen of the usual Slater-Jastrow form, $\Psi(R)=D(R)J(R)$, where $R\equiv(\mathbf{r}_1,\ldots,\mathbf{r}_N)$ represents the coordinates of the N electrons. The Jastrow factor is a pair product, $J(R)=\exp[-\Sigma_{i<j}u(r_{ij})]$, with $u(r)$ as the parameter-free RPA pseudopotential.[15] The phase structure is fixed by the complex factor $D=\Pi_\nu D_\nu$, i.e., a product of Slater determinants, one for each spin-valley component.

Most of the simulations were carried out with the standard PW choice for the one-particle orbitals, $D_\nu^{\mathrm{PW}}=\det[\exp(i\mathbf{k}_i\cdot\mathbf{r}_j)]$. For $\zeta=0$ and $\zeta=1$ we also included BF correlations,[14] $D_\nu^{\mathrm{BF}}=\det[\exp(i\mathbf{k}_i\cdot\mathbf{x}_j)]$, where $\mathbf{x}_i=\mathbf{r}_i+\Sigma_{j\neq i}^N\eta(r_{ij})(\mathbf{r}_i-\mathbf{r}_j)$ and the BF function $\eta(r)$ (of the form suggested in Ref. 14) was optimized by minimization of the variational energy.

We simulated the imaginary-time evolution of the system by a branching random walk using a short-time approximation of the importance-sampled Green's function and exerting control on the number of walkers. Calculations were performed at $r_s=1,2,5,10,20,40$. For $\zeta=0$ and $\zeta=1$ we chose several values of the number of electrons between $N=36$ and $N=116$, whereas 11 intermediate values of the polarization, defined by flipping one spin at a time, were studied for $N=52$. The twist average, for the PW simulations, was performed on a mesh defined by $q_x(i)=\Delta(i-1/2)$, $q_y(j)=\Delta(j-1/2)$, $1\leq i\leq 8$, $i\leq j\leq 8$, $\Delta=\pi/8L$, with L the side of the simulation box. Long-range interactions were dealt with the optimized-splitting method of Ref. 37.

Extrapolation to zero time step τ and infinite number of walkers N_W was also carried out at fixed density, on the assumption that the τ and N_W dependences are approximately independent. Results at polarizations $\zeta=0$, $\zeta\simeq 0.5$, and $\zeta=1$, and for a bunch of τ (N_W) values were used to establish the τ (N_W) dependence of the energy as function of ζ; these dependences, combined together, were then used to extrapolate to $N_W=\infty$, $\tau=0$ the energies calculated for all values of ζ.

We record the difference between BF and PW energies at zero and full polarizations in Table II, and the whole set of energies extrapolated to $N_W=\infty$, $\tau=0$, and including the backflow correction in Table III.

TABLE III. Data used for the fit described in the paper. Twist-averaged DMC energy in Rydberg per particle $E_N(r_s,\zeta)$, calculated at finite N, extrapolated to zero time step and infinite number of walkers, and including BF correlations; in parentheses the statistical error on the last two figures are shown. The backflow correction was calculated using the largest N entries of Table II (for given density and polarization).

r_s	N	ζ	$E_N(r_s,\zeta)$	r_s	N	ζ	$E_N(r_s,\zeta)$	r_s	N	ζ	$E_N(r_s,\zeta)$
1	36	0	−0.76940(15)	5	36	0	−0.308540(26)	20	36	0	−0.0930324(80)
	36	1	−0.42501(21)		36	1	−0.299849(46)		36	1	−0.092705(13)
	52	0	−0.76418(14)		52	0	−0.308001(25)		42	1	−0.092681(13)
	52	1/13	−0.76192(14)		52	1/13	−0.307933(26)		52	0	−0.0929597(79)
	52	2/13	−0.75430(15)		52	2/13	−0.307727(26)		52	1/13	−0.0929559(80)
	52	3/13	−0.74537(15)		52	3/13	−0.307614(27)		52	2/13	−0.0929483(81)
	52	4/13	−0.73040(15)		52	4/13	−0.307191(28)		52	3/13	−0.0929498(83)
	52	5/13	−0.71189(16)		52	5/13	−0.306660(29)		52	4/13	−0.0929340(85)
	52	6/13	−0.68872(16)		52	6/13	−0.305994(31)		52	5/13	−0.0929046(87)
	52	7/13	−0.66258(17)		52	7/13	−0.305416(33)		52	6/13	−0.0928788(91)
	52	8/13	−0.63301(17)		52	8/13	−0.304745(35)		52	7/13	−0.0928636(96)
	52	9/13	−0.59922(18)		52	9/13	−0.303896(37)		52	8/13	−0.092842(10)
	52	10/13	−0.55908(19)		52	10/13	−0.302872(39)		52	9/13	−0.092816(11)
	52	11/13	−0.51827(19)		52	11/13	−0.301915(42)		52	10/13	−0.092765(11)
	52	1	−0.42381(21)		52	1	−0.299624(46)		52	11/13	−0.092735(12)
	84	0	−0.76258(14)		84	0	−0.307778(25)		52	1	−0.092659(13)
	84	1	−0.42201(21)		84	1	−0.299197(45)		84	0	−0.0929138(79)
									84	1	−0.092577(13)
									100	1	−0.092562(13)
2	26	3/13	−0.587078(70)	10	26	3/13	−0.172824(16)		116	1	−0.092552(13)
	36	0	−0.590629(64)		36	0	−0.172782(15)				
	36	1	−0.51883(12)		36	1	−0.171014(29)				
	52	0	−0.588677(63)		42	1	−0.171000(29)	40	36	0	−0.0489598(23)
	52	1/13	−0.588144(63)		50	1	−0.170903(29)		36	1	−0.0488830(31)
	52	2/13	−0.586577(65)		52	0	−0.172599(15)		52	0	−0.0489302(23)
	52	3/13	−0.584820(67)		52	1/13	−0.172555(15)		52	1/13	−0.0489325(23)
	52	4/13	−0.581489(70)		52	2/13	−0.172524(15)		52	2/13	−0.0489275(23)
	52	5/13	−0.577593(76)		52	3/13	−0.172522(16)		52	3/13	−0.0489312(24)
	52	6/13	−0.572603(79)		52	4/13	−0.172425(17)		52	4/13	−0.0489244(24)
	52	7/13	−0.567330(85)		52	5/13	−0.172309(18)		52	5/13	−0.0489179(24)
	52	8/13	−0.561367(91)		52	6/13	−0.172163(19)		52	6/13	−0.0489100(25)
	52	9/13	−0.554274(96)		52	7/13	−0.172056(20)		52	7/13	−0.0489053(26)
	52	10/13	−0.54584(10)		52	8/13	−0.171941(21)		52	8/13	−0.0489042(27)
	52	11/13	−0.53737(11)		52	9/13	−0.171760(23)		52	9/13	−0.0488968(27)
	52	1	−0.51815(12)		52	10/13	−0.171525(24)		52	10/13	−0.0488833(28)
	78	3/13	−0.583684(65)		52	11/13	−0.171362(26)		52	11/13	−0.0488779(29)
	78	7/13	−0.566625(84)		52	1	−0.170929(29)		52	1	−0.0488635(31)
	84	0	−0.587940(61)		78	3/13	−0.172383(16)		78	7/13	−0.0488920(26)
	84	1	−0.51703(12)		78	7/13	−0.171970(20)		84	0	−0.0489127(23)
	104	7/13	−0.566206(83)		84	0	−0.172490(15)		84	1	−0.0488322(31)
					84	1	−0.170718(29)		104	7/13	−0.0488743(26)
					90	1	−0.170765(29)				
					104	7/13	−0.171901(20)				

APPENDIX B: HIGH- AND LOW-DENSITY LIMIT OF THE CORRELATION ENERGY OF THE FOUR COMPONENT 2DEG

We directly refer to Ref. 17 for both the $r_s \to \infty$ limit, whose leading terms in r_s^{-1} and $r_s^{-3/2}$ are independent of the number of components,[38] and the $r_s \to 0$ limit at $\zeta=1$, which is the same two-component system as the one-valley case at $\zeta=0$.[17]

Here we only need to specify the high-density limit for the four-component system, $\lim_{r_s \to 0} e_c(r_s,0)=A_0+B_0 r_s \ln r_s$. Generalizing the procedure of Ref. 39 to the multivalley case, we write e_c as the sum of the second-order exchange energy $e_2^{(b)}$ and the ring contribution $e_c^{(r)}$, whose lowest order $e_2^{(r)}$ is the direct term of the second-order energy per particle. It turns out that $e_2^{(b)}$ is a constant, independent of r_s and the number of components of the system, N_c, while $e_2^{(r)} = e_2^{(r)}(N_c)$ depends only on N_c. Furthermore, we notice that the ring contribution scales with N_c as $e_c^{(r)}(r_s,N_c) = N_c f(r_s N_c^{3/2})$, so that the following scaling law holds:

$$e_c^{(r)}(r_s,4) = 2e_c^{(r)}(4\sqrt{2}r_s,2). \tag{B1}$$

By applying the scaling law [Eq. (B1)] to the leading terms of e_c, we find $A_0=e_2^{(b)}+2e_2^{(r)}(2)=-0.99870$ and $B_0=16(10-3\pi)/(3\pi)$.

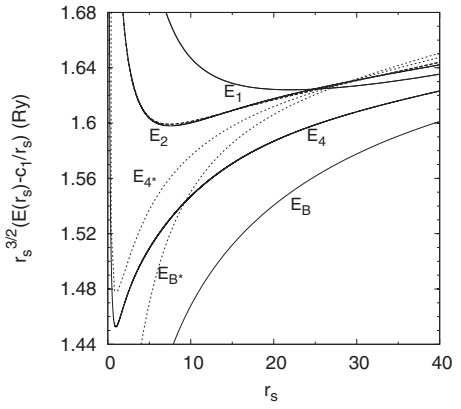

FIG. 3. Phase diagram of the multicomponent 2DEG: liquid phases. Solid E_4 and E_2 from the present work, solid E_1 and long dashed E_2 from Ref. 17, and E_B from Ref. 28. E_{4^*} and E_{B^*} are from Ref. 31. One- and two-component energies from Ref. 31 coincide with the ones in Ref. 17 by construction.

APPENDIX C: CHECK OF AN APPROXIMATE MULTICOMPONENT CORRELATION ENERGY

In Fig. 3 we show a comparison between the multicomponent correlation energy $\tilde{\epsilon}_c(N_c)$ of Ref. 31 and various simulation results, including the present two-valley calculation, and the nominally exact QMC results for charged bosons.[28] Total energies are displayed. The scale of the figure emphasizes the limited accuracy of $\tilde{\epsilon}_c(N_c)$ in the large r_s regime.

[1] *Semiconductor Spintronics and Quantum Computing*, edited by D. D. Awscholom, N. Samarth, and D. Loss (Springer-Verlag, Berlin, 2002).
[2] P. Simon and D. Loss, Phys. Rev. Lett. **98**, 156401 (2007).
[3] A. A. Shashkin, S. Anissimova, M. R. Sakr, S. V. Kravchenko, V. T. Dolgopolov, and T. M. Klapwijk, Phys. Rev. Lett. **96**, 036403 (2006), and references therein.
[4] O. Gunawan, Y. P. Shkolnikov, K. Vakili, T. Gokmen, E. P. De Poortere, and M. Shayegan, Phys. Rev. Lett. **97**, 186404 (2006), and references therein.
[5] V. M. Pudalov, M. E. Gershenson, H. Kojima, N. Butch, E. M. Dizhur, G. Brunthaler, A. Prinz, and G. Bauer, Phys. Rev. Lett. **88**, 196404 (2002).
[6] S. V. Kravchenko and M. P. Sarachik, Rep. Prog. Phys. **67**, 1 (2004), and references therein.
[7] S. Anissimova, S. V. Kravchenko, A. Punnoose, A. M. Finkel'stein, and T. M. Klapwijk, Nat. Phys. **3**, 707 (2007).
[8] T. Ando, A. B. Fowler, and F. Stern, Rev. Mod. Phys. **54**, 437 (1982).
[9] S. Conti and G. Senatore, Europhys. Lett. **36**, 695 (1996).
[10] A. Punnoose and A. M. Finkel'stein, Science **310**, 289 (2005).
[11] O. Gunawan, T. Gokmen, K. Vakili, M. Padmanabhan, E. P. De Poortere, and M. Shayegan, Nat. Phys. **3**, 388 (2007).
[12] See, e.g., G. Giuliani and G. Vignale, *Quantum Theory of the Electron Liquid* (Cambridge University Press, Cambridge, 2005).
[13] B. Tanatar and D. M. Ceperley, Phys. Rev. B **39**, 5005 (1989).
[14] Y. Kwon, D. M. Ceperley, and R. M. Martin, Phys. Rev. B **48**, 12037 (1993).
[15] F. Rapisarda and G. Senatore, Aust. J. Phys. **49**, 161 (1996).
[16] D. Varsano, S. Moroni, and G. Senatore, Europhys. Lett. **53**, 348 (2001).
[17] C. Attaccalite, S. Moroni, P. Gori-Giorgi, and G. B. Bachelet, Phys. Rev. Lett. **88**, 256601 (2002).
[18] S. De Palo, M. Botti, S. Moroni, and G. Senatore, Phys. Rev. Lett. **94**, 226405 (2005), and references therein.
[19] Y. Zhang and S. Das Sarma, Phys. Rev. B **72**, 075308 (2005).
[20] Y. Zhang and S. Das Sarma, Phys. Rev. B **72**, 115317 (2005).
[21] M. W. C. Dharma-wardana and F. Perrot, Phys. Rev. B **70**, 035308 (2004).
[22] Indeed, for the one-valley 2DEG the RPA grossly overestimates χ_s (Ref. 40) and predicts a divergence at moderately low density (Ref. 20) which can only be ascribed to its limited accuracy. Similarly, a small but unjustified change in the correlation energy in the calculations carried out for the 2V2DEG within the classical mapping changes a χ_s finite and smooth at all densities in a diverging one.
[23] M. Foulkes, L. Mitas, R. J. Needs, and G. Rajagopal, Rev. Mod. Phys. **73**, 33 (2001).
[24] C. Lin, F. H. Zong, and D. M. Ceperley, Phys. Rev. E **64**, 016702 (2001).
[25] Evidently, we disregard the valley splitting predicted when going beyond the effective-mass approximation (Ref. 8).

[26] G. Ortiz, D. M. Ceperley, and R. M. Martin, Phys. Rev. Lett. **71**, 2777 (1993).
[27] F. H. Zong, C. Lin, and D. M. Ceperley, Phys. Rev. E **66**, 036703 (2002).
[28] S. De Palo, S. Conti, and S. Moroni, Phys. Rev. B **69**, 035109 (2004).
[29] Further energy gain for the four-component phase could be in principle obtained by allowing spin/valley contamination, i.e., considering a spin/valley dependent backflow. However, a systematic study exploiting this possibility (Ref. 41) for the unpolarized three-dimensional electron gas gave energies in error bar with ones obtained with spin-independent backflow (Ref. 42).
[30] K. Kärkkäinen, M. Koskinen, S. M. Reimann, and M. Manninen, Phys. Rev. B **70**, 195310 (2004).
[31] K. Kärkkäinen, M. Koskinen, S. M. Reimann, and M. Manninen, Phys. Rev. B **68**, 205322 (2003).
[32] Actually, the convexity of $E(r_s,\zeta)$ is spoiled by the exchange term at some finite polarization ζ_c. However, for $r_s \gtrsim 1$, correlation effects push ζ_c exponentially close to one, in a range $1-\zeta_c \propto e^{-\beta r_s}$.
[33] Y. Zhang and S. Das Sarma, Phys. Rev. Lett. **96**, 196602 (2006).
[34] A. A. Shashkin, A. A. Kapustin, E. V. Deviatov, V. T. Dolgopolov, and Z. D. Kvon, Phys. Rev. B **76**, 241302(R) (2007).
[35] A. A. Shashkin, M. Rahimi, S. Anissimova, S. V. Kravchenko, V. T. Dolgopolov, and T. M. Klapwijk, Phys. Rev. Lett. **91**, 046403(R) (2003).
[36] T. Gokmen, M. Padmanabhan, E. Tutuc, M. Shayegan, S. De Palo, S. Moroni, and G. Senatore, Phys. Rev. B **76**, 233301 (2007).
[37] V. Natoli and D. M. Ceperley, J. Comput. Phys. **117**, 171 (1995).
[38] The coefficients of the leading powers of r_s are kept fixed to their analytical values for the crystal phase in Ref. 17, whereas they are fitting parameters in the present work.
[39] A. Rajagopal and J. C. Kimball, Phys. Rev. B **15**, 2819 (1977).
[40] S. De Palo, G. Senatore, M. Botti, and S. Moroni, Phys. Rev. Lett. **97**, 039702 (2006).
[41] P. López Ríos, A. Ma, N. D. Drummond, M. D. Towler, and R. J. Needs, Phys. Rev. E **74**, 066701 (2006).
[42] M. Holzmann, D. M. Ceperley, C. Pierleoni, and K. Esler, Phys. Rev. E **68**, 046707 (2003).